

# Preparation of Silicon Carbide Powder with Ultra-Wide Particle Size Range and Controllable Morphology

Shengyuan Xu<sup>1, 2</sup>, Shibo Guo<sup>\*1</sup>, Weiyou Yang<sup>2</sup>, Feng Hu<sup>\*2</sup>

<sup>1</sup>School of Materials Science and Engineering, Hunan University of Science and Technology, Xiangtan, 411201, China.

<sup>2</sup>Institute of Micro/Nano Materials and Devices, Ningbo University of Technology, Ningbo, 315211, China.

received April 13, 2024; received in revised form November 12, 2024; accepted November 18, 2024

## Abstract

Nanoscale( $D_{50} = 83$  nm), microscale( $D_{50} = 32$   $\mu$ m), and millimeter-scale( $D_{50} = 0.3$  mm) pure phase  $\beta$ -SiC powders were synthesized through a two-step self-propagating high-temperature synthesis (SHS) method in an argon atmosphere, utilizing spherical-like graphite as the source materials with varied particle sizes. Accordingly, these spherical SiC powders were efficiently fabricated on a large scale by coating carbon spheres with molten silicon. It is found that the SiC powders are predominantly influenced by the characteristics of the carbon source employed, leading to their controllable growth in particle size and morphology based on a typical vapor-solid (V-S) mechanism. In such process, the carbon particles are enclosed by liquid silicon within the reactive units, thus effectively maintaining their inherent morphology and size. This mechanism allows for strategic manipulation of the granularity and shape of SiC powders by varying the carbon feedstock.

*Keywords:* Silicon carbide, self-propagating high temperature synthesis, controlled growth

## I. Introduction

Silicon carbide, as a third-generation semiconductor material for electronic devices, exhibits high strength, exceptional hardness, outstanding wear resistance, a large bandgap, high breakdown field strength, and excellent oxidation resistance<sup>1-3</sup>. The development of silicon carbide ceramics and third-generation semiconductor materials heavily relies on the use of silicon carbide powders with adjustable particle sizes and controllable morphologies<sup>4-6</sup>. Different morphologies and particle sizes of silicon carbide, such as nanoparticles, nanotubes, and nanowires/spherical forms, are widely applied in energy storage and conversion, sensors, photodetectors, and other fields due to their unique physical and chemical properties<sup>7-11</sup>. And silicon carbide powders with a broad range of particle sizes and a relatively uniform size distribution offer more extensive and practical applications. Thus, a comprehensive exploration of the controlled preparation of silicon carbide powders exhibiting different particle sizes and morphologies holds significant importance in advancing the performance and applications of silicon carbide ceramics and semiconductor materials.

The fabrication of SiC powder encompasses several methodologies, broadly categorized into solid-phase, liquid-phase, and gas-phase methods<sup>12-14</sup>. The liquid-phase method (such as the sol-gel method) for preparing

SiC offers advantages like high powder purity and uniform particle size distribution. However, as this method typically operates in an organic liquid-phase environment, both the Si and C sources are derived from organic compounds, which can easily produce harmful substances, posing risks to human health and the environment and hindering sustainable ecological development. In contrast, the gas-phase method (CVD method) typically requires high-purity gaseous Si and C sources. This leads to high raw material costs, while the SiC powder produced is of low yield and challenging to collect, making it difficult to meet the demands of the semiconductor industry. Solid-phase techniques, exemplified by the Acheson method, offer notable advantages in terms of cost-effectiveness and high production yields<sup>15</sup>. However, despite their widespread adoption due to these merits, solid-phase methods present challenges in precisely controlling particle size and morphology, often requiring substantial energy input and long reaction times. Additional solid-phase approaches involve high-temperature decomposition and combustion synthesis. Notably, combustion synthesis has emerged as a cost-effective means for SiC powder production<sup>16</sup>. Yet, due to the exothermic nature of the SiC synthesis reaction, sustaining continuous reactions necessitates auxiliary measures such as preheating<sup>14</sup>, the addition of combustion aids<sup>17</sup>, and reactions within a nitrogen atmosphere<sup>18</sup>. Unfortunately, these measures may introduce complications, such as impurity phases and environmental concerns during silicon carbide powder production. Conversely, the high-temperature self-

\* Corresponding author: [guoshibo163@163.com](mailto:guoshibo163@163.com)  
co-corresponding author: [hfl7@tsinghua.org.cn](mailto:hfl7@tsinghua.org.cn)

propagation method, facilitated by externally supplied thermal energy, ensures the stable production of specific crystal-phase mono-phase SiC powder. While liquid-phase and gas-phase methods offer effective control over SiC powder particle size, they entail lower yields and a restricted adjustable range of particle size, typically within the nanometer scale. During the self-propagating high-temperature reaction, the adiabatic temperature frequently surpasses the melting point of silicon. In the silicon-carbon system, the reaction predominantly involves liquid-solid and gas-solid interactions. Therefore, we first keep the temperature at the liquidus temperature of silicon (1400 °C) to allow the molten silicon particles to coat the carbon source, and then continue to raise the temperature to allow the Si source and C source to react continuously to form SiC. The two-step method can be used to prepare SiC powder using the carbon source as a template. By changing the morphology and particle size of the carbon raw material, we can effectively control the morphology and particle size of the SiC<sup>16</sup>. Consequently, manipulating the morphology and particle size of SiC crystals becomes feasible based on alteration of the morphology and particle size of the carbon raw material.

This investigation details the synthesis of  $\beta$ -SiC powders, ranging from nano to millimeter scale, with near-spherical morphology, with a two-step, high-temperature self-propagating method under an argon gas environment using diverse carbon precursors. Furthermore, it delves into the controlled growth mechanisms of silicon carbide at temperatures exceeding 1400 °C.

## II. Experimental Procedure

The raw materials include commercial Si powder (purity >99.99 %,  $D_{50} = 7 \mu\text{m}$ , China); nanometer carbon black (purity >99 %,  $D_{50} = 50 \text{ nm}$ , marked as C-1, Henan Delong carbon black, China); micronmeter graphite (purity >99 %,  $D_{50} = 30 \mu\text{m}$ , marked as C-2, China); millimeter graphite (purity >99 %,  $D_{50} = 0.5 \text{ mm}$ , marked as C-3, Sinopharm Group, China); multi-walled carbon

nanotubes carbon (purity >99 %,  $D_{50} = 80 \text{ nm}$ , marked as C-4, Sinopharm Group, China); active carbon (purity >99 %,  $D_{50} = 3 \mu\text{m}$ , marked as C-5, Henan Delong carbon black, China); spherical graphite (purity >99 %,  $D_{50} = 12 \mu\text{m}$ , marked as C-6, China). In addition, to make sure there is no excess silicon in the reactants, the Si:C was designed as 1.2:1, the raw materials were used in a simple mix, and then loaded in a porous graphite crucible, which was placed into a tube furnace. Subsequently, the tube furnace was filled with high-purity Ar<sub>2</sub> to an ordinary pressure, gas flow as 260. Silicon carbide powder was synthesized using a two-step self-propagating high-temperature synthesis method. Initially, the temperature was rapidly increased to 1400 °C, below the melting point of silicon, and maintained for 2 hours to facilitate the initial nucleation of silicon carbide. Subsequently, the temperature was raised to 1500 °C at a rate of 3 K/min and held for 5 hours. Finally, the sample underwent heat treatment in a muffle furnace at 800 °C in an air atmosphere for 3 hours, resulting in single-phase silicon carbide powder. The sample was then collected after cooling to room temperature.

The crystalline phases of the products were identified by means of X-ray diffraction (XRD, D8 Advance, Bruker, Germany). The microstructure was observed by means of field-emission scanning electron microscope (SEM, S-4800, Hitachi, Japan). Energy-dispersive X-ray spectroscopy mapping (EDS; ESCALAB 250Xi, Thermo Fisher, USA) was used to evaluate the elemental distribution. The average particle size of  $\beta$ -SiC was obtained by measurement and statistics from SEM images, with at least 100 particles being measured for each sample.

## III. Results and Discussion

The X-ray diffraction (XRD) patterns and Raman spectra of the synthesized products, derived from various carbon sources, are illustrated in Fig. 1 (SC1 – SC6). The use of carbon sources with different initial particle sizes and morphologies enabled the successful synthesis of  $\beta$ -SiC.

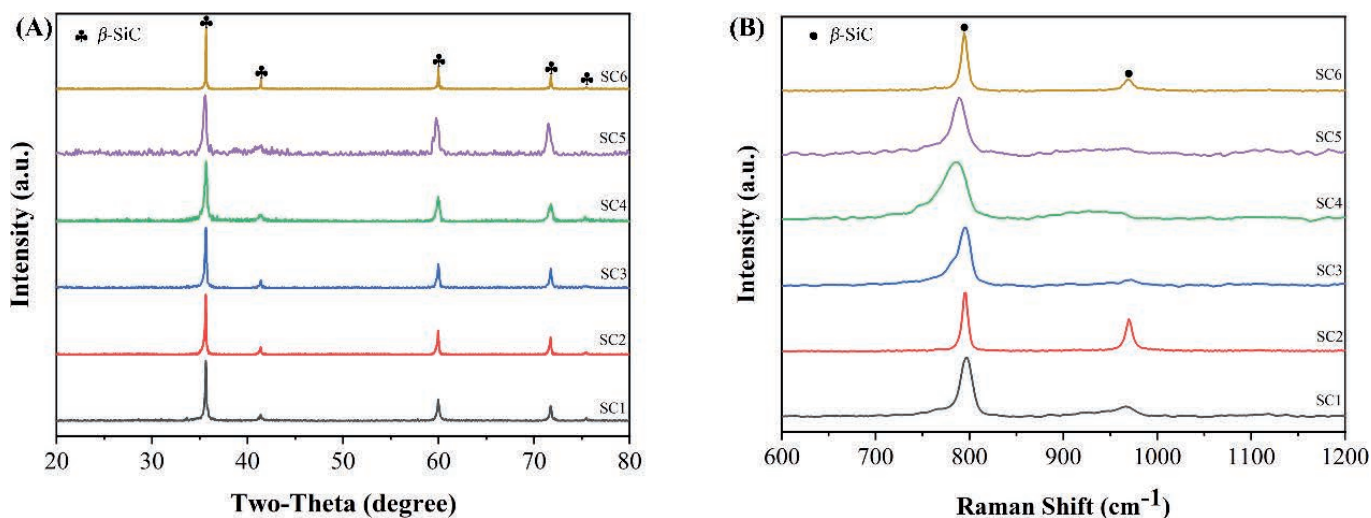
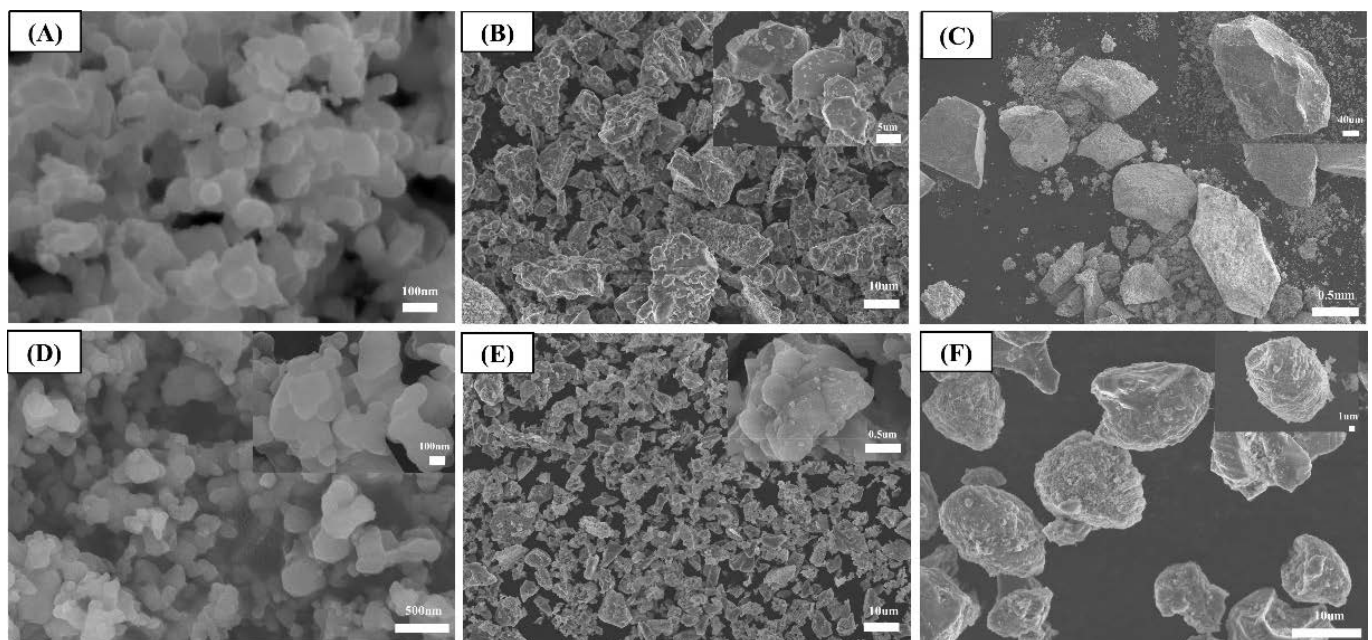


Fig. 1: (A) X-ray diffraction patterns of the combustion (B) Raman diffraction patterns of the combustion.

Post-heat treatment analysis showed no traces of residual silicon phases or carbon peaks, confirming the purity of the  $\beta$ -SiC phases. This purity was consistently achieved regardless of the carbon source's particle size and morphology, indicating the stability of the phase composition of the products. A complete conversion to monophasic  $\beta$ -SiC was facilitated by increasing the carbon-to-silicon molar ratio and implementing a secondary sintering process. This method negated the need for extended mixing, or the addition of combustion aids and activators, thus presenting an efficient pathway for the complete transformation of raw materials into monophasic  $\beta$ -SiC. Utilizing carbon sources of varying sizes, including nanometer, micrometer, and millimeter scales, resulted in the preparation of respective  $\beta$ -SiC sizes. The XRD analysis revealed that when nanometer-sized carbon black was used as the carbon source, the XRD pattern of the combustion products exhibited significant noise. This observation can be attributed to the amorphous nature of carbon black, its high defect concentration, and its strong tendency to agglomerate. These characteristics may lead to localized agglomeration during the self-propagating reaction, resulting in an uneven reaction process and poor crystallinity in the resulting SiC powder<sup>16, 19</sup>. Raman spectroscopic analysis (SC1-SC6) identified characteristic peaks at 796 and 972  $\text{cm}^{-1}$  in the combustion-synthesized silicon carbide powder. The peak at 796  $\text{cm}^{-1}$  corresponds to the transverse optical phonon mode, while the peak at 972  $\text{cm}^{-1}$  is associated with the longitudinal optical phonon mode of  $\beta$ -SiC. Importantly, the absence of residual carbon and silicon peaks further corroborates the purity of the synthesized product. The employed two-step sintering process incorporates a low-temperature holding stage, facilitating solid-state reactions between carbon and silicon, which promote the nucleation of silicon carbide. The subsequent gradual temperature increase allows for the controlled and uniform growth of silicon carbide crystal nu-

clei. This methodology ensures the even occurrence of the self-propagating high-temperature synthesis, culminating in the formation of impurity-free, monophasic  $\beta$ -SiC.

Fig. 2 and Fig. 3 show Scanning Electron Microscopy<sup>19</sup> images and Energy Dispersive Spectroscopy (EDS) spectra of silicon carbide powders synthesized from varied carbon sources. Table 1 lists the average particle sizes of  $\beta$ -SiC. Utilizing nano-sized carbon black as the carbon source resulted in the preparation of mono-phase nano-sized SiC powder. Conversely, employing micron-sized graphite as the carbon source yielded mono-phase micron-sized SiC powder. Additionally, millimeter-sized mono-phase SiC powder was synthesized using millimeter-sized activated carbon. The SEM images reveal that the silicon carbide possesses a distinct crystalline structure devoid of residual silicon and carbon impurities. Fig. 2 depicts silicon carbide particles synthesized in various sizes. It is apparent that modifying the granularity of the carbon source leads to proportional adjustments in silicon carbide particle size. Subfigures D, E, and F represent the synthesized silicon carbide powders associated with different carbon source morphologies. The manipulation of carbon source morphology induces corresponding alterations in silicon carbide powder morphology, with Subfigure D showing a nanotubular morphology, Subfigure E exhibiting a layered morphology, and Subfigure F presenting a near-spherical morphology. Fig. 3 displays the EDS spectra of SC3, SC4, and SC5, demonstrating a uniform distribution of silicon and carbon elements. It is evident that, with the silicon source unchanged, significant differences exist in the morphology of the synthesized silicon carbide powders. SC4 silicon carbide particles exhibit a tubular surface structure, whereas SC5 silicon carbide particles display a flake-like structure. SC6 exhibits a near-spherical structure. The morphologies of the synthesized silicon carbide powders align with those of the carbon sources.



**Fig. 2:** Scanning electron microscope images of the reaction-produced silicon carbide powder: (A) SC-1 (B) SC-2 (C) SC-3 (D) SC-4 (E) SC-5 and (F) SC-6.



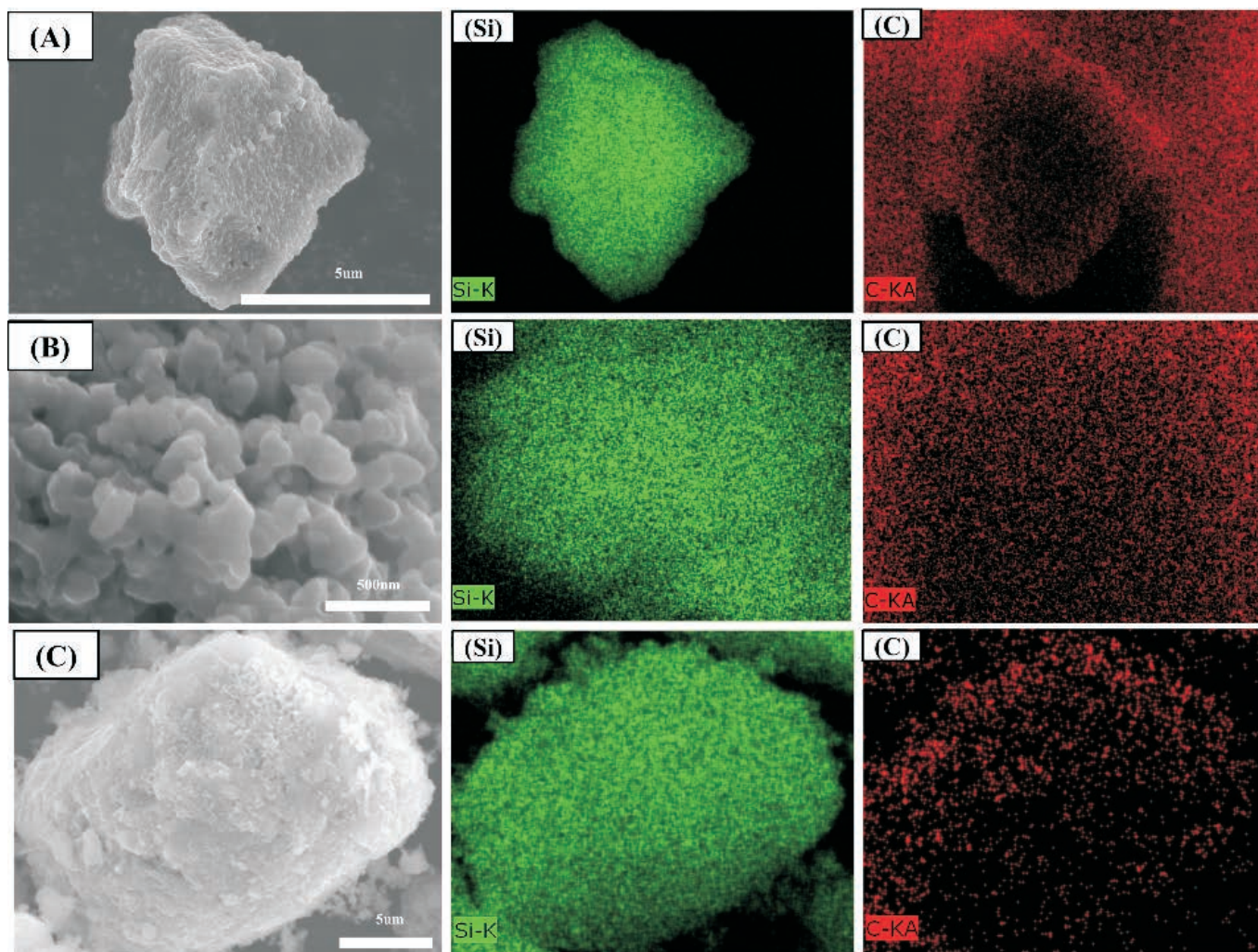


Fig. 3: The energy-dispersive X-ray spectroscopy (EDS) images of the reaction-produced silicon carbide powder: (A) SC-5 (B) SC-4 (C) SC-6.

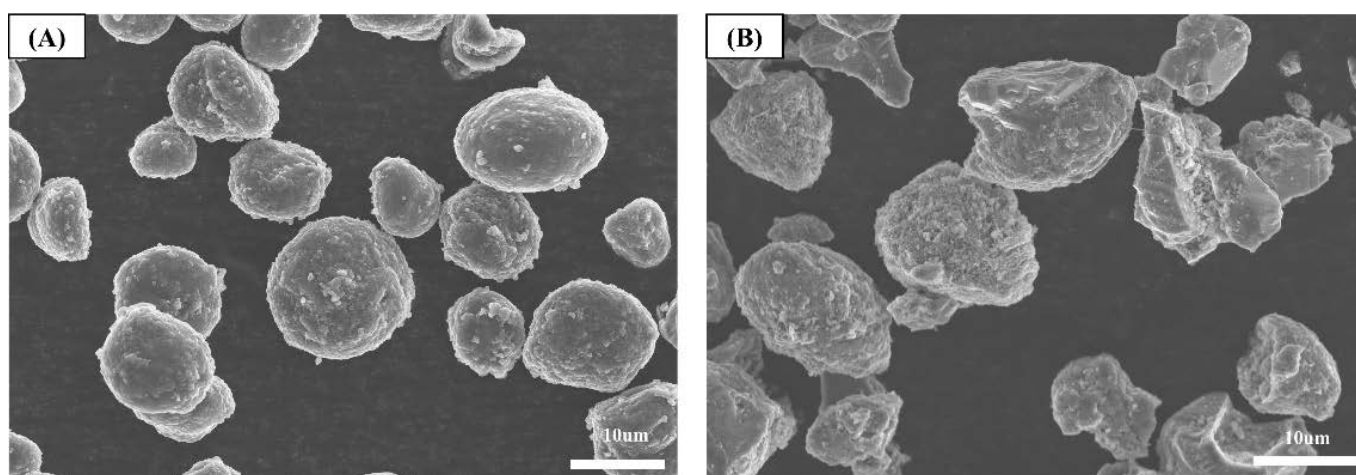


Fig. 4: The scanning electron microscope images of the pre-reaction carbon source and post-reaction silicon carbide particles: (A) Pre-reaction carbon source of SC-6 (B) Post-reaction silicon carbide particles of SC-6.

It is important to note that the particle size of the synthesized silicon carbide is not significantly influenced by the original silicon powder. Instead, it predominantly inherits its characteristics from the initial carbon source. For instance, when carbon nanotubes served as the carbon source, nano-tubular silicon carbide powder was produced, with a particle size similar to the original nan-

otubes. This observation suggests that the carbon source retains its nanotube structure throughout the high-temperature conversion process to SiC. The data presented in Fig. 4 clearly indicate that throughout the silicon carbide powder synthesis process in SC6, the morphology and particle size of the resultant silicon carbide particles maintain consistency with the characteristics of the initial car-

bon source. As the process progresses through the high-temperature holding stage, there is noticeable growth in the silicon carbide particles, leading to slight irregularities in morphology. However, the overall appearance remains predominantly near-spherical, showing excellent flowability without any observed aggregation phenomenon.

Furthermore, when micron-sized spherical graphite was employed as the carbon source, the resulting product was micron-sized spherical mono-phase SiC particles. This finding demonstrates that the morphology and particle size of silicon carbide synthesized during the high-temperature self-propagating synthesis process are largely determined by the characteristics of the original carbon source. Utilizing carbon sources as templates in the high-temperature self-propagation method sheds light on effective strategies for controlling the morphology and particle size of silicon carbide.

In the self-propagating synthesis of silicon carbide powder at temperatures above 1400 °C, the process entails silicon liquefaction and slight gasification, attributable to its melting point being in excess of 1420 °C<sup>20</sup>. This phenomenon results in a solid-liquid reaction where liquid silicon droplets, displaying fluidity, are capable of encapsulating carbon particles. During the isothermal holding at 1500 °C, SiC nucleation and growth transpire regionally through a dissolution-diffusion mechanism. Here, liquid silicon persistently reacts with the surface of carbon particles, infiltrating their interiors driven by capillary forces<sup>21, 22</sup>. Within each reaction zone, the process culminates as carbon particles are entirely converted into SiC. SEM and EDS analyses confirm that the particle size and morphology of the resulting silicon carbide are influenced by the dimensions and structure of the initial carbon material. With the meticulous selection of carbon powders of varying sizes, silicon carbide powders ranging from nanoscale to millimeter-scale were synthesized. Notably, employing micron-sized spherical graphite powder facilitated the synthesis of micrometer-sized spherical silicon carbide powder. Due to the encapsulation of liquid silicon on the surface of spherical graphite, a silicon-coated carbon structure is formed. As the duration of heat treatment is increased, silicon continuously reacts with carbon to form a silicon carbide layer, progressively diffusing into the interior of the spherical graphite. Eventually, this leads to the complete conversion into spherical silicon carbide.

The synthesis of silicon carbide powders with varied particle size distributions is depicted in Fig. 5. The results clearly demonstrate that using carbon sources of three different sizes directly correlates with the sizes of the resultant silicon carbide powders. In detail, nano-sized carbon sources facilitated the production of mono-phase silicon carbide powder with a median diameter ( $D_{50}$ ) of 83 nm. In contrast, micron-sized carbon sources led to the formation of mono-phase silicon carbide powder with a  $D_{50}$  of 32  $\mu\text{m}$ , while millimeter-sized carbon sources resulted in mono-phase silicon carbide powder with a  $D_{50}$  of 0.31 mm. Notably, all three particle sizes of silicon carbide powders exhibit relatively narrow distributions in their respective size ranges.

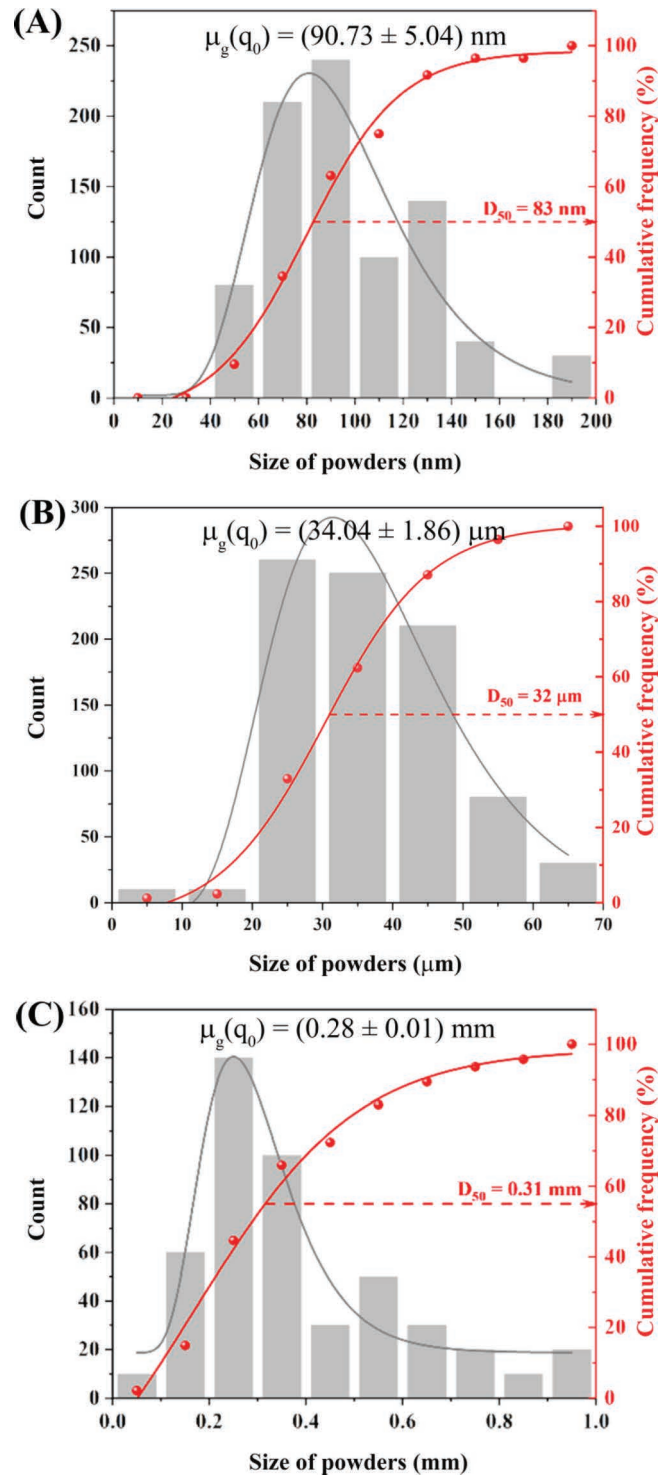


**Fig. 5:** Particle size distribution of reaction-produced silicon carbide powder. (A) Nanoscale silicon carbide powder (B) Micron silicon carbide powder (C) Millimeter silicon carbide powder.

A comparison of the particle sizes of the synthesized silicon carbide powders with those of the original carbon sources reveals distinct trends. The particle size distribution of the original carbon source can be seen in Fig. S1. For nano-sized carbon sources, an increase in the particle size of the resultant silicon carbide was observed post the self-propagating high-temperature synthesis. This contrasts with the results from micron-sized and millimeter-sized carbon sources, which yielded a reduction in the silicon carbide particle size, as detailed in Table 1. This trend



**Table 1:** The particle size of raw materials and reaction products.

Sample	Si	C	Phase assemblage	Particle size of $\beta$ -SiC
SC-1	Si-1 (7 $\mu\text{m}$ )	C-1 (50 nm)	$\beta$ -SiC	83 nm
SC-2	Si-1 (7 $\mu\text{m}$ )	C-2 (30 $\mu\text{m}$ )	$\beta$ -SiC	32 $\mu\text{m}$
SC-3	Si-1 (7 $\mu\text{m}$ )	C-3 (0.5 mm)	$\beta$ -SiC	0.31 mm
SC-4	Si-1 (7 $\mu\text{m}$ )	C-4 (80 nm)	$\beta$ -SiC	0.16 $\mu\text{m}$
SC-5	Si-1 (7 $\mu\text{m}$ )	C-5 (3 $\mu\text{m}$ )	$\beta$ -SiC	2.27 $\mu\text{m}$
SC-6	Si-1 (7 $\mu\text{m}$ )	C-6 (12 $\mu\text{m}$ )	$\beta$ -SiC	12 $\mu\text{m}$

suggests that during the self-propagating high-temperature synthesis for silicon carbide, a general contraction occurs, leading to a decrease in particle size. However, the nano-sized carbon black, known for its higher reactivity, triggers a faster reaction. The extended exposure to high temperatures in this scenario promotes grain growth and may lead to aggregation, thus contributing to an increase in the silicon carbide particle size.

#### IV. Conclusions

By employing the high-temperature self-propagating method in a flowing argon atmosphere, we successfully synthesized single-phase silicon carbide across nano, micro, and millimeter scales. This resulted in uniformly distributed, sphere-like silicon carbide powders. The powders were synthesized using nano carbon black, micrometer graphite, and millimeter activated carbon as the carbon sources. When nano carbon black was utilized, the resultant single-phase silicon carbide powder had an average particle size of 83 nm. Similarly, using micrometer graphite as the carbon source led to single-phase silicon carbide powder with an average particle size of 32  $\mu\text{m}$ . The use of millimeter activated carbon as the raw material yielded larger particles, resulting in millimeter-scale single-phase silicon carbide powder. Notably, the employment of spherical graphite as a template facilitated the synthesis of spherical-like silicon carbide powder. The silicon carbide synthesis process involved a combination of dissolution precipitation and gas-solid reactions, with the final morphology and particle size primarily determined by the precursor carbon particles. Thus, selecting an appropriate precursor carbon source is crucial for controlling the final morphology and particle size of the synthesized silicon carbide powder.

In the self-propagating synthesis of silicon carbide powder at temperatures exceeding 1400  $^{\circ}\text{C}$ , the reaction includes the liquefaction and slight gasification of silicon, which has a melting point above 1420  $^{\circ}\text{C}$ . This leads to a solid-liquid reaction where liquid silicon droplets, exhibiting fluidity, encapsulate the carbon particles. During the isothermal holding at 1500  $^{\circ}\text{C}$ , SiC nucleation and growth occur through a dissolution-diffusion mechanism. The liquid silicon reacts continuously with the surface of carbon particles and diffuses into their interiors, driven by capillary forces. The reaction within each zone concludes once carbon particles are completely transformed into SiC. SEM and EDS observations reveal that the particle size and morphology of silicon carbide depend on the car-

bon raw material's size and morphology. By manipulating carbon powders of various sizes, we prepared silicon carbide powders in nano-scale, micrometer-scale, and millimeter-scale. Particularly, the use of micron-sized spherical graphite powder led to the synthesis of micrometer-sized spherical silicon carbide powder. This method can effectively regulate the particle size distribution and morphology of  $\beta$ -SiC powder, which will be beneficial to research and application in the semiconductor and functional ceramic fields.

#### Acknowledgments

This work was supported by the National Natural Science Foundation of China (NO. 52302067), State Key Laboratory of New Ceramic and Fine Processing Tsinghua University (NO. KF202315), Ningbo University of Technology Scientific Research Foundation Project (NO. 3090011540001), Ningbo University of Technology research and cultivation project (NO. 0080011560275).

#### References

- Ackley, B.J., Martin, K.L., Key, T.S.: Advances in the synthesis of preceramic polymers for the formation of silicon-based and ultrahigh-temperature non-oxide ceramics, *Chem. Rev.*, **123**, [8], 4188–4236, (2023).
- Chabi, S., Kadel, K.J.N.: Two-dimensional silicon carbide: emerging direct band gap semiconductor, *Nanomaterials.*, **10**, [11], 2226, (2020).
- Rai, P., Kim, Y-S., Kang, S-K., Yu, Y-T.: Synthesis of nano-sized silicon carbide through non-transferred arc thermal plasma, *Plasma Chem. Plasma P.*, **32**, 211–8, (2012).
- Liu, J., Xiao, H., Guo, W., Gao, P., Liang, J.: Spheroidization of SiC powders and their improvement on the properties of SiC porous ceramics, *Ceram. Int.*, **44**, [4], 3830–3836, (2018).
- Wang, T., Gong, W., He, X.: Synthesis of highly nanoporous  $\beta$ -silicon carbide from corn stover and sandstone, *ACS Sustainable Chem. Eng.*, **8**, [39], 14896–14904, (2020).
- Amirkhanyan, N., Kirakosyan, H., Zakaryan, M., Zurnachyan, A., Rodriguez, M., Abovyan, L., Aydinyan, S.: Sintering of silicon carbide obtained by combustion synthesis, *Ceram. Int.*, **49**, [15], 26129–26134, (2023).
- Chen, S., Li, W., Li, X., Yang, W.: One-dimensional SiC nanostructures: designed growth, properties, and applications, *Prog Mater Sci.*, **104**, 138–214, (2019).
- Nehra, M., Dilbaghi, N., Marrazza, G.: 1D semiconductor nanowires for energy conversion, harvesting and storage applications, *Nano Energy*, **76**, 104991, (2020).
- Lan, X., Wang, Z.J.C.: Efficient high-temperature electromagnetic wave absorption enabled by structuring binary porous SiC with multiple interfaces, *Carbon.*, **170**, 517–526, (2020).

- 10 Feng, W., Ma, J., Yang, W.J.C.: Precise control on the growth of SiC nanowires, *CrystEngComm.*, **14**, [4], 1210–1212,(2012).
- 11 Chen, J., Zhang, B., Xu, D., Yu, Z., He, G.: Influence of heat treatment of amorphous Ti-and B-containing SiC-based fiber in air on microstructure and strength, *J. Ceram. Sci. Technol.*, **9**, 279–288, (2018).
- 12 Najafi, A., Fard, F.G., Rezaie, H.R., Ehsani, N.: Synthesis and characterization of SiC nano powder with low residual carbon processed by sol-gel method, *Powder Technol.*, **219**, 202–210, (2012).
- 13 Fraga, M., Pessoa, R.: Progresses in synthesis and application of SiC Films: from CVD to ALD and from MEMS to NEMS, *Micromachines Basel.*, **11**, [9], 799, (2020).
- 14 Mukasyan, A.S., Lin, Y.C., Rogachev, A.S., Moskovskikh, D.O.: Direct combustion synthesis of silicon carbide nanopowder from the elements, *J. Am. Ceram. Soc.*, **96**, [1], 111–117, (2013).
- 15 Pramono, A., Dhoska, K., Moezzi, R., Milandia, A.: Ti/SiC based metal matrix composites by using self-propagating high temperatures synthesis (SHS), *Rev. Compos. Mater. Av.*, **31**, [3], 125–129, (2021).
- 16 Li, F., Cui, W., Tian, Z., Zhang, J., Du, S., Chen, Z., Chen, K., Liu, G.: Controlled growth of SiC crystals in combustion synthesis, *J Am Ceram Soc.*, **105**, [1], 44–49, (2021).
- 17 Hao, L.U.O., Xuqing, Z., Deren, Y.: Research progress on high-purity SiC powder for single crystal SiC growth, *J. Syn. Cryst.*, **50**, [8], (2021).
- 18 Krasovskii, P.V., Samokhin, A.V., Kirpichev, D.E.: Carbon forms, carbide yield and impurity-driven nonstoichiometry of plasma-generated  $\beta$ -silicon carbide nanopowders, *Mater. Chem. Phys.*, **25**, [3], 123077, (2020).
- 19 Zeraati, M., Kazemzadeh, P., Barani, M., Sargazi, G.J.S.: Selecting the appropriate carbon source in the synthesis of SiC nano-powders using an optimized fuzzy model, *Silicon-Neth.*, 1–12, (2021).
- 20 Manocha, L.M., Prasad, G., Manocha, S.: Synthesis and characterization of carbon-silicon carbide particulate composites by powder metallurgical route, *Int. J. Appl. Ceram. Tec.*, **19**, [1], 119–129, (2022).
- 21 Zhou, X.N., Hao, X., Xu, J.Q.: Light-weight, wood-derived, biomorphic SiC ceramics by carbothermal reduction, *Ceram. Int.*, **50**, [13], 23135–23149, (2024).
- 22 Duan, X., Lu, S., Jiang, X.: Preparation of silicon carbide powder from amorphous silica and investigation of synthesis mechanism, *Minerals*, **14**, [2], 189, (2024).

## Supporting Information

## Preparation of Silicon Carbide Powder with Ultra-wide Particle Size Range and Controllable Morphology

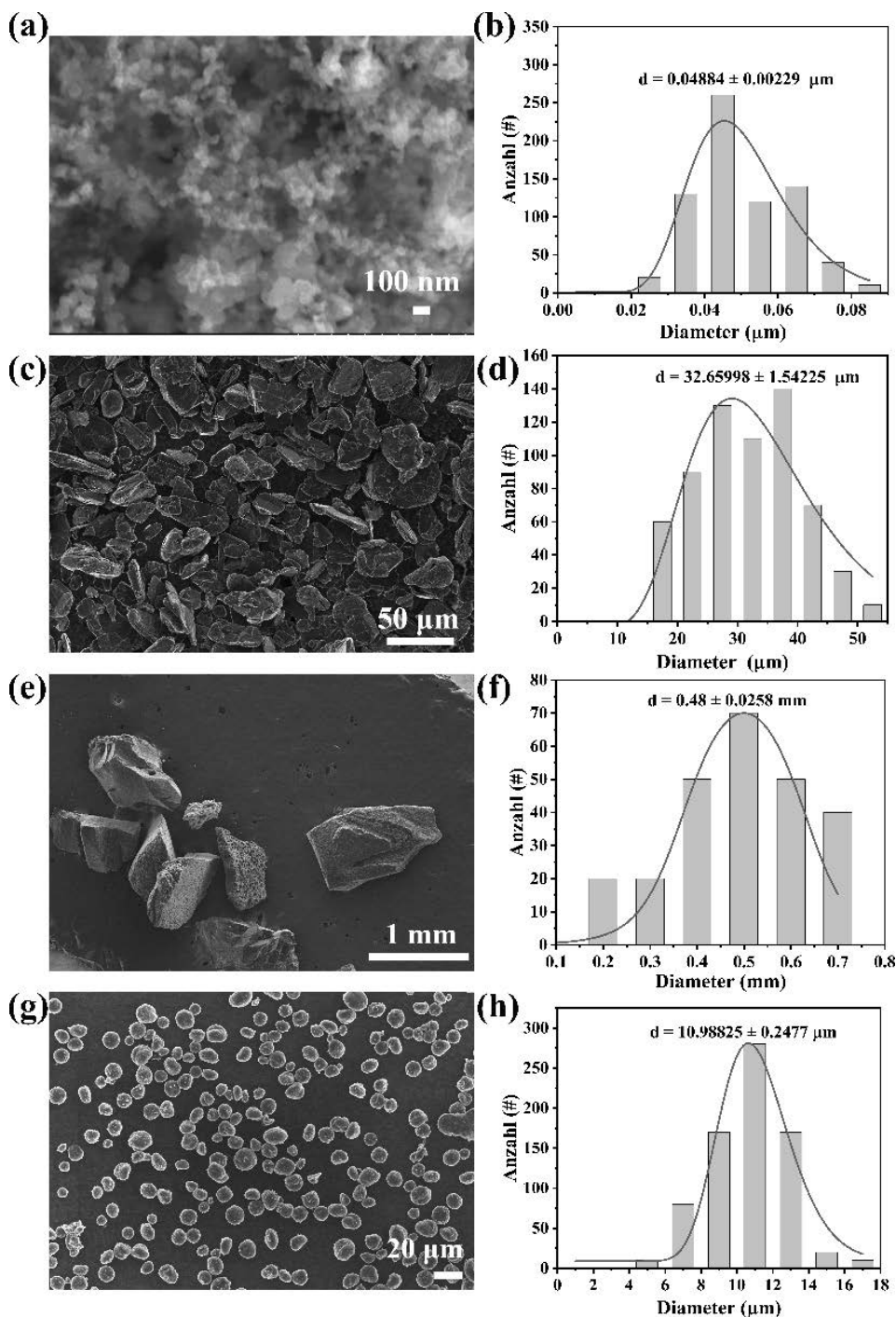
Shengyuan Xu<sup>1, 2</sup>, Shibo Guo<sup>\*1</sup>, Weiyu Yang<sup>2</sup>, Feng Hu<sup>\*2</sup><sup>1</sup>School of Materials Science and Engineering, Hunan University of Science and Technology, Xiangtan, 411201, China.<sup>2</sup>Institute of Micro/Nano Materials and Devices, Ningbo University of Technology, Ningbo, 315211, China.

Fig. S1: (a-b) SEM image of nanocarbon source and its particle size distribution. (c-d) SEM image of micron carbon source and its particle size distribution. (e-f) SEM image of millimeter-scale carbon source and its particle size distribution. (g-h) SEM image of spherical carbon source and its particle size distribution.



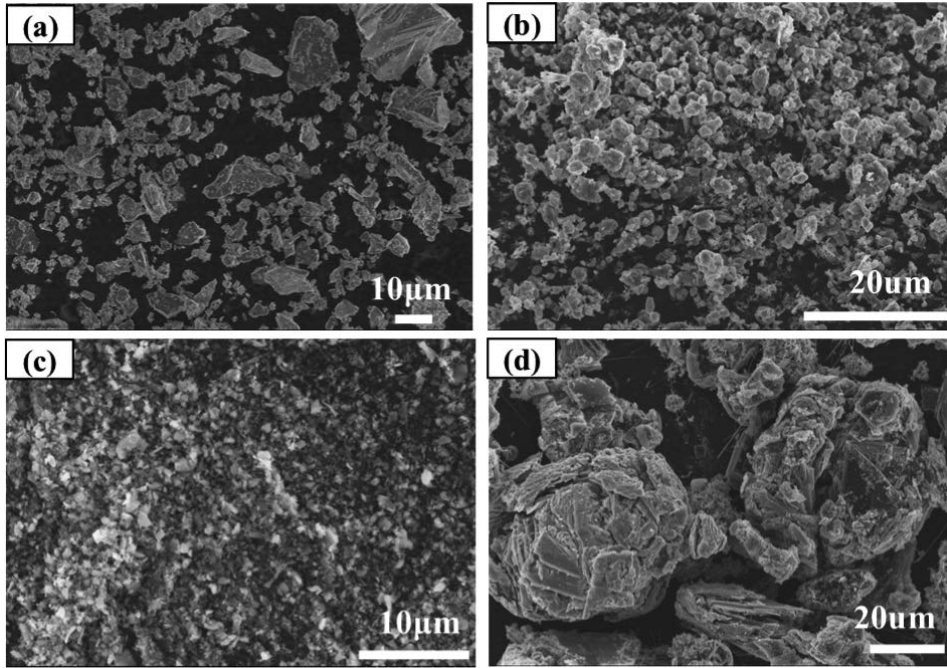


Fig. S2: (a-b) Micron-sized silicon powder and its preparation to obtain SiC powder. (c-d) Submicron silicon powder and its preparation to obtain SiC powder.

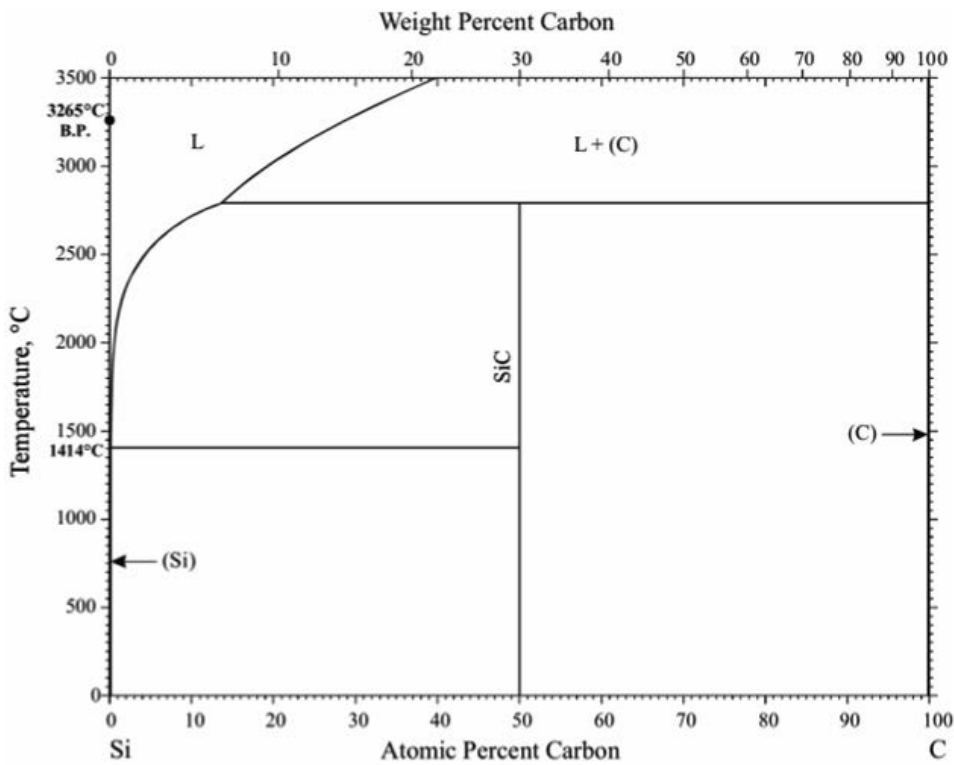


Fig. S3: C-Si binary phase diagram <sup>1</sup>

Reference

<sup>1</sup> Okamoto H.: Supplemental Literature Review of Binary Phase Diagrams: Ag-Li, Ag-Sn, Be-Pu, C-Mn, C-Si, Ca-Li, Cd-Pu, Cr-Ti, Cr-V, Cu-Li, La-Sc, and Li-Sc, *JPED*, 38(1), 70-81,( 2017).

